30th NENE 2021
September 6 - 9
BLED-SLOVENIA
International Conference Nuclear Energy for New Europe

Experimental exploration of interweaved fluctuations of pressure and velocity in 5x5 rod bundle with spacer grids

Naz Turankok[1, 2], Lionel Rossi [1]
CEA Cadarache
[1] DES/IRESNE/DTN/STCP, [2]l'Université Paris Saclay
13115 Saint-Paul-lez-Durance, FRANCE
Naz.turankok@cea.fr, lionel.rossi@cea.fr

Thibaud Lohez[1], Valerie Biscay[1]
CEA Cadarache
[1] DES/IRESNE/DTN/STCP
13115 Saint-Paul-lez-Durance, FRANCE
Thibaud.LOHEZ@cea.fr, valerie.biscay@cea.fr

ABSTRACT

In Pressurized Water Reactor (PWR) core, the fuel assemblies are made of fuel rods maintained by spacer grids. With the aging of the spacer grids, the fluid-structure interactions provoke vibrations leading to fretting by contacts between the rods and grid elements. This fretting is one of the major reason for the degradation of the outer layer of the fuel rods. To explore the origins of the local excitations of the rods by the flow, analytical experiments are performed with an experimental low-pressure water rig, named CALIFS, which consists in a 5x5 rod bundle maintained with analytical spacer-grids. Previous measurements, [1] show the existence of frequency peaks in pressure fluctuations spectra downstream spacer grids (with and without mixing vanes) for a Reynolds number of 66000. In a recent article, using rods with Fluorinated ethylene propylene (FEP) parts to perform Particle Image Velocimetry (PIV) measurements close to the central instrumented rod, [2] highlight the flow phenomena plausibly responsible for the frequency peaks. The presence of coherent vortex streets is observed by Laser Doppler Velocimetry (LDV) and PIV measurements. Current work includes PIV measurements for configuration with and without mixing vane. For the quantification of the transport of pressure and velocity fluctuations, simultaneous pressure and PIV measurements are performed using multi-pressure sensors devices. These results show that the pressure fluctuations are correlated with structures that are observed in PIV measurements and convected with the speed of flow.

1 INTRODUCTION

The fuel assemblies are found inside the core of Pressurized Water Reactors (PWR) with the coolant flow. These fuel assemblies are composed by fuel rods and hold by spacer grids. With the coolant flow where Reynolds number can reach up to 500000 [3], vibrations on the rods can be observed within fuel assemblies. These vibrations are generated by the fluid-structure interactions promoted by the turbulent flow within the rod bundles and the additional source of turbulence supplied by the spacer grids. With the aging of the grid, fretting on the rods occurs due to the contacts between the rods and the grid elements. This fretting is named grid-to-rod fretting. This phenomenon is one of the major reason for the degradation of the outer

layer of the fuel rods which can lead to damaged rods [4]. Experimental studies are performed to support the validation of Computational Fluid Dynamics (CFD) simulations and to estimate the forces exerted on the rods. These studies are performed with the support of the "FUEL ASSEMBLY Project" (FRAMATOME, CEA, EDF). In addition, it is expected that the combination of such refined experiments and CFD simulations will support the characterisation of the hydraulic performance of the grids.

Different experimental studies can be found in the literature regarding the measurements of the flow inside fuel assemblies with methods such as Laser Doppler Velocimetry (LDV) [5] and Particle Image Velocimetry (PIV) [6] [7] using Refractive Index Method (RIM). These studies provides a database for CFD simulations [8] and can be found for different arrays of rods bundle and different configurations of grids.

The experimental low-pressure water rig, named CALIFS is used for the investigation of flow within 5x5 rod bundle. In previous experiments, [1] [2] a frequency peak is observed on the pressure spectra for a broad range of Reynolds numbers (13000-108000) for configuration with and without mixing vane, i.e. WMV and NMV respectively, which reveals a periodicity inside the flow. The LDV measurements [2], show the existence of frequency peak downstream of the grid elements, i.e. dimples and springs, with a higher turbulent energy distribution downstream the dimples. For this cause this manuscript mainly focuses on the flow region downstream the dimples. To find the source of this periodicity, PIV measurements are performed downstream the dimples using Refractive Index Method (RIM). The first result of High-speed PIV shows that the coherent structures persist downstream the grid, making eddy streets, for the Reynolds number 13800 – 19300 [2].

To investigate the interconnection between the pressure fluctuations and the velocity fluctuations the experiments are repeated with simultaneous pressure and PIV measurements. This manuscript presents new results obtained by High-speed PIV for WMV and NMV, Low-Speed PIV and the preliminary results of simultaneous measurements for NMV configuration.

2 EXPERIMENTAL APPARATUS AND MEASUREMENTS

2.1 Description of the experimental rig

MERCURE 400 is a water experimental facility supplying different rigs dedicated to the study of turbulent flows within rod bundles. The working ranges are 0-400m3/h for the flowrate and 12°C-55°C for the temperature which is regulated with heat exchanger. The rig CALIFS 5x5 is connected to MERCURE 400. Figure 1(a) and (b) shows the 3D schematics and photo of CALIFS, respectively. The vertical length of CALIFS is about 2.5m. It has optical access (Perspex windows) on three sides. CALIFS has a square array (184mm on each side) where a 5x5 rod bundle is inserted. The rods made of INOX tube with a diameter of 26.7mm. Compared to PWR, the scale of CALIFS is 2.81 which facilitates the spatial resolution of the measurements. The hydraulic diameter is defined as $D_h = 27.7mm$. The effect of the wall is minimised around the central rod of CALIFS within a central zone with 3x3 rods as shown in the Figure 1(c). The flow around the central rod is representative of the flow in larger arrays. In this zone, the geometric diameter is defined as $D_G = 1.21D_h$. The shortest distance is the gap between two rods which is 8.9mm and the Pitch-to-diameter ratio (P/D) is 1.33.

The Reynolds number of the flow inside CALIFS is given by Eq. (1) where ν [m²/s] is the kinematic viscosity.

$$Re_{D_h} = U_{flow} * D_h/\nu \tag{1}$$

To maintain the rod bundle, four spacer-grids are used inside CALIFS. These grids are analytical up-scaled spacer-grids with a simplified design. This design is aimed to reproduce

key features of fuel assemblies' grids. In Figure 2(a), these spacer-grids are numbered from 1 to 4. Spacer-grids 1 and 4 are without mixing vanes to maintain the rods of the extremity of the test section. Spacer-grids 2 and 3 are with No Mixing Vanes (NMV) or With Mixing Vanes

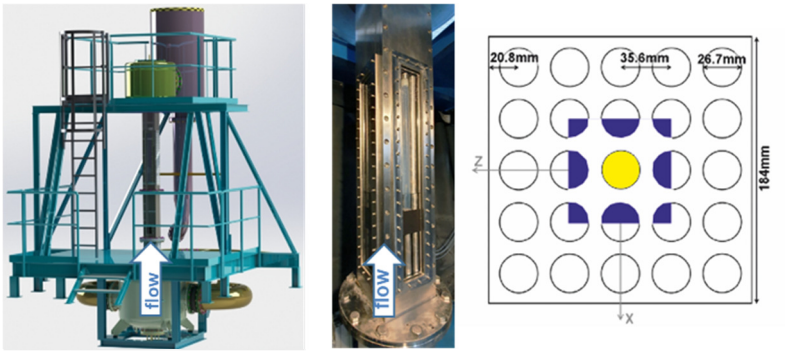

Figure 1: (a) 3D illustration CALIFS 5x5 rig (b) Photo of the test section (c) Top view of the rod bundles where yellow circle represents the selected rod and the blue part represents zone minimized from the wall effect

(WMV) depending on the measurements which are illustrated in Figure 2(b).

More details about the rig and the grids design are given in [1].

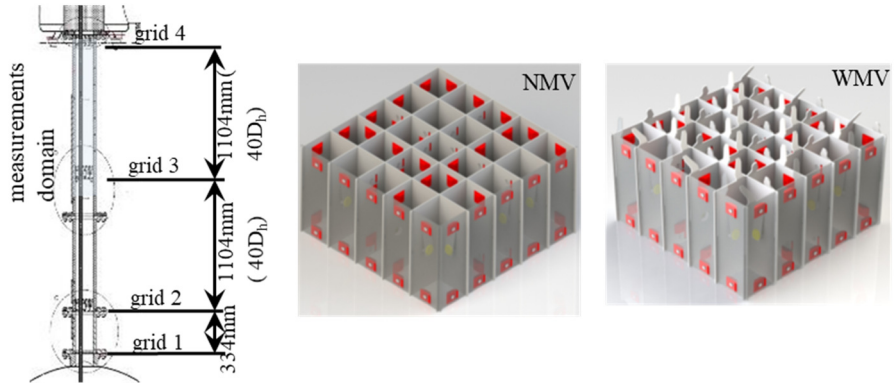

Figure 2: Schematics of test section and schematics of grids without mixing vane (NMV) and with mixing vane (WMV)

2.2 Measurements

Figure 3 (a) presents a graphical summary of the experiments performed.

For local pressure measurements, a multisensor device is used by four KULITE XCL-072 brand pressure sensors with a diameter of 1.9mm. These sensors are mounted flush to the wall/flow with 0.5Dh distance between each other to measure the pressure fluctuations instantaneously. Figure 3(b) shows the multisensor device which is installed in the central rod with the angular position of interest. The recording performed at 10kHz for 60s using a 1 kHz low pass analogue filter. The uncertainty of pressure measurements is observed to be about 4 Pa or 8% whichever is the higher. More details can be found in [1]. Pressure fluctuations are defined as $P' = P - \overline{P}$ where $\overline{P}$ represents the temporal average of the local pressure. Energy spectra are computed using 3sec duration windows spaced by 1sec. A mobile average over 11 points (1Hz window) is applied to the spectra. Power spectra are normalised by the total energy.

For the velocity measurements PIV is performed with the implementation of RIM to have optical access of the measurement domain, i.e. near the central rod. RIM decreases the optical distortions due to the refraction and/or reflection of the light at the interface of two media [9]

For the application of RIM, two INOX rod are replaced with transparent FEP (Fluorinated Ethylene Propylene) rod where the application can be seen on Figure 3(c). More details about material selection can be found in [2].

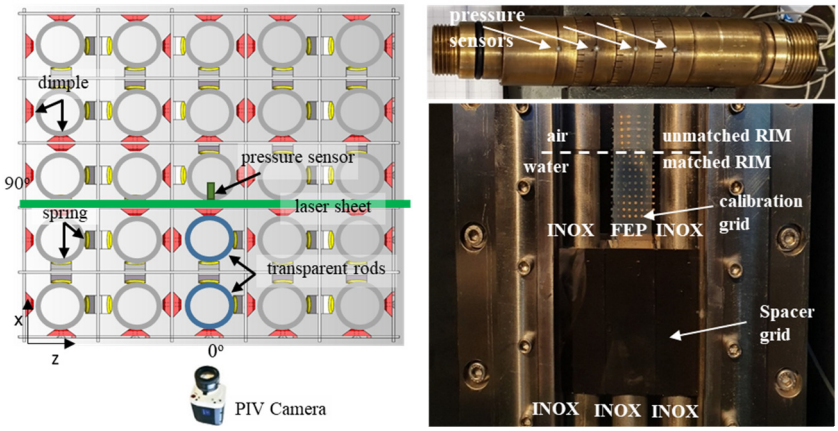

Figure 3: (a) Implementation of measurements techniques (b) Multisensor device (c) RIM application in CALIFS 5x5

PIV measurements are performed with various range of Reynolds Number using two different PIV configurations, i.e. High-speed PIV and Low-speed PIV. Measurement domain is selected as 2mm away from the wall of the central rod where the dimple is positioned. The calibration process is performed with a calibration grid which gives the opportunity to ensure the position of the camera, the laser and the laser sheet. For both configurations, the camera and the laser are placed perpendicularly to each other and the laser sheet is then placed in front of the central rod with an accuracy of ±0.1mm. The thickness of the laser light sheet is checked to be about 1mm. More details about the calibration can be found in [2]. After the calibration procedure, the central rod is placed back and the particles are added to the flow. The displacements are computed with LaVision PIV software (DaVis 10.1.2).

For High-speed PIV, the displacements are calculated between frames k and k+3 and an extra time filter is applied on the results i.e. smoothing frequencies above 1kHz. For both High-speed and Low-speed PIV 3x3 spatial smoothing (mobile average) is applied to the data.

For the simultaneous measurements to investigate the connection between pressure fluctuations and velocity fluctuations, the pressure measurements are simultaneously performed with PIV measurements. The pressure sensors are aligned with a spacing of $0.5D_h$ and are installed from $y = 0D_h$, i.e. same level as top of spacer grid. The sensors are placed at 20°. This angle is chosen according to the maximum pressure and velocity fluctuations [1] [2]. Details about PIV part of the measurements can be found in Table 1.

Table 1: Summary of measurement characteristics for PIV

	Experimental campaigns		
	Only PIV		PIV and pressure
Type of PIV	High-speed PIV	Low-speed PIV	High-speed PIV
Camera	Phantom Miro Lab110, 1280pix x 800pix at 1690Hz, 12bit	LaVision Imager SX 9M, 3360pix x 2712pix at 18frame/s, 8/12bit	Phantom Miro Lab110, 1280pix x 800pix at 1690Hz, 12bit
Laser	532nm Nd:YAG continuous laser	532nm Nd:YAG pulse laser (200mJ, 15Hz)	532nm Nd:YAG continuous laser
Velocity range	0.5m/s-0.7m/s	0.5m/s-2.8m/s	0.5m/s-0.9m/s
Temperature	20°C	12°C-55°C	12°C-55°C
Particle type	PMMA-Rhodamine B-Particles	PMMA-Rhodamine B-Particles	Vestosint 2070 + Sulforhodamine B
Particle diameter	1-20µm	1-20µm	10µm
Particle density	1.18(g/cm3)	1.18(g/cm3)	1.19(g/cm3)
Recording Frequency	5044Hz	15Hz	3982Hz
Total Frames	25727	5000	20040
Maximum displacement	12pxl-14pxl	20pxl	12pxl-14pxl
Measurement domain	0Dh-1.4Dh	0Dh-2.21Dh ; 3Dh-5.21Dh	0Dh-2Dh
Spatial Resolution (pxl/mm)	17.76 pxl/mm	54.67 pxl/mm; 40.45 pxl/mm	18.77 pxl/mm

For the post-processing, to achieve the same recoding rate as PIV data i.e. 3982Hz, mobile averaged pressure signal is resampled by 2nd order interpolation. For the recording of the simultaneous measurements, in-house LABVIEW code is developed and connected with DAVIS software by PTU-X hardware. To ensure the simultaneousness of pressure measurements and PIV measurements, time information of recordings is registered by LABVIEW.

3 RESULTS AND DISCUSSIONS

Previous measurements [2] presented High-speed PIV results for Re=16500 with NMV configuration. In these results, the coherent structures are observed with the presence of a wake downstream the dimples. These structures are observed to persist up to $y/D_h = 1.4$ for a range of Reynolds numbers between 13800 – 19300. The shear layers are observed between low and high velocity zones and the maximum fluctuations are found in the shear layer on the two sides of the dimple.

Figure 4 shows the preliminary High-speed PIV results for Re=19300 with WMV configuration where the mixing vanes are marked with black rectangles. Figure 4(a) shows the instantaneous dimensionless velocity intensity with the streamlines in the reference frame of the laboratory, i.e. velocity components u and v. Figure 4(b) shows the swirling function, S^*, calculated similarly to [2] [10]. The streamlines are plotted in the reference frame of the mean flow, i.e. with u-U_{flow} and v. Figure 4(c) shows the mean velocity field ($\|\bar{U}\|/U_{flow}$). The root mean square of the velocity fluctuations is defined as u'_{RMS} and u'_{RMS}/U_{flow} is presented in Figure 4(d). U_{flow} is defined as the mean velocity of the flow within the rod bundle.

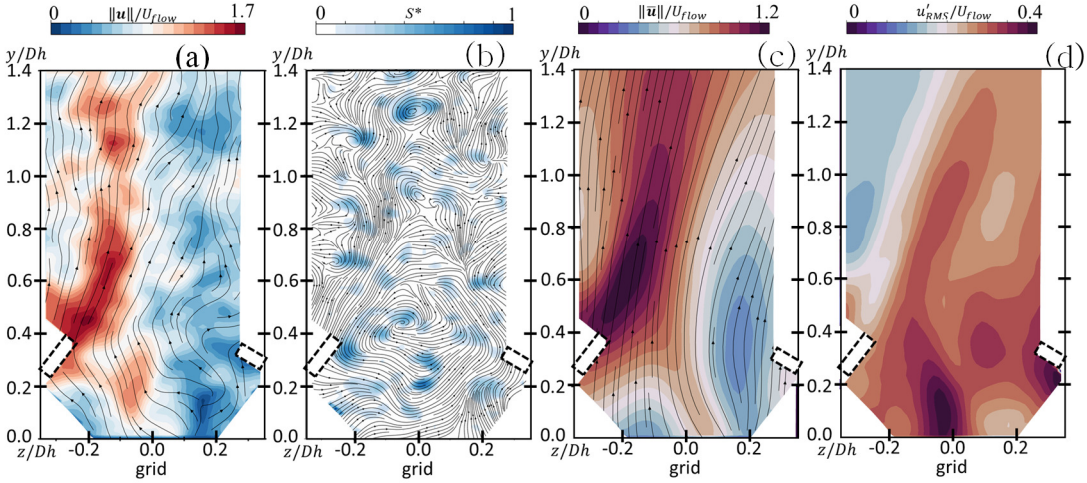

Figure 4: Velocity results for $Re_{D_h} = 19300$ (a) instantaneous velocity field and streamlines (b) swirling function with streamlines in the mean frame of the flow (c) averaged velocity intensity and streamlines (d) $\boldsymbol{u'_{RMS}}$

The effect of the mixing vane is observed on the preliminary results of WMV configuration as illustrated in Figure 4(a) and (c). Compared to NMV configuration [2], with the effect of the mixing vane, the high velocity zone can be seen between $z/D_h = -0.3$ to the centre of the dimple, i.e. $z/D_h = 0$, and low velocity zone is observed on the other side of the dimple, i.e. $z/D_h = 0 - 0.2$. The shear layer that can be observed on both sides of the dimple with NMV configuration is observed to be shifted with WMV configuration. The coherent structures can be seen in the centre, downstream of the dimple where for NMV configuration it is observed on both sides of the dimple. These structures are observed to persist up to $y/D_h = 1.4$. The Figure 4(d) shows the velocity fluctuations for WMV configuration which are observed to be maximum downstream the dimple where the shear layer is observed and the

high fluctuation zone is observed to stay up to $y/D_h = 1.4$ which start to shift after $y/D_h = 0.6$.

Figure 5(a) and (b) shows two characteristic time scales that are calculated from real time PIV data for NMV configuration. These are the integral length scale which represents the size of the structures and the periodic length scale which represents the distance between periodic structures. The integral length scale, L_i is calculated by using autocorrelation function on velocity points. The positions are selected according to where the structures are observed, i.e. z/Dh=0.2.

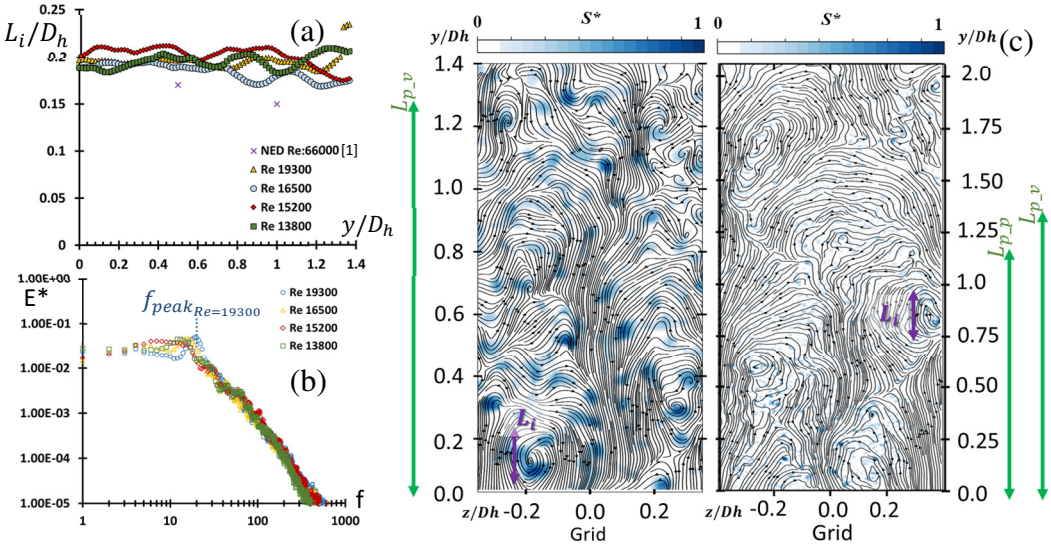

Figure 5: (a) Integral length scale for z/Dh=0.2 for $Re_{D_h} = 13800 - 66000$ (b) Normalized velocity spectra $Re_{D_h} = 13800 - 19300$ (c) Snapshot of swirling function for $Re_{D_h} = 13800$ and $Re_{D_h} = 66000$

Figure 5(a) shows the integral length scale for Reynolds number 13800-66000, which includes L_i calculated by using pressure fluctuations [1]. The velocity integral length scales vary between 0.19Dh-0.21Dh and is about constant with the increased distance from the grid. This is in agreement with the pressure integral length scale. Figure 5(b) shows the frequency peak, f_{peak} which is used to define the periodic length scale L_{p_v}, i.e. U_{flow}/f_{peak}. Figure 5(c) shows a snapshot of swirling function for Re_{D_h}=13800 with High speed PIV and Re_{D_h}=66000 with Low speed PIV. The scales represented for High-speed PIV are 0.19Dh for L_i and 1.21Dh for L_{p_v}. For Low speed PIV, scales represented according to the LDV and pressure measurements [1] [2] as 0.18Dh for L_i, 1.32Dh and 1.16Dh for L_{p_v} and L_{p_p} respectively for velocity and pressure fluctuations. For both results, calculated scales are observed to be coherent with the structures observed on the PIV results.

To summarize the results, Strouhal-Reynolds map is built. It highlights the relation between the flow and the observed frequencies. The Strouhal number is calculated as [2]. Figure 6 shows the updated map for with and without mixing vane configuration. The plot includes pressure measurements, LDV measurements and High-speed PIV measurements. From the graph a relation between Reynolds and Strouhal is observed for both velocity and pressure fluctuations where Strouhal number varies between 0.20 and 0.26. The results shows that the phenomena is represented by the coherent structures and can be observed on both pressure fluctuations and velocity fluctuations.

To investigate the relation between the velocity and pressure fluctuations, simultaneous measurements are performed. Cross-correlation method is performed with the velocity data that is obtained by the High-speed PIV and the pressure data that is obtained from the multi-sensor

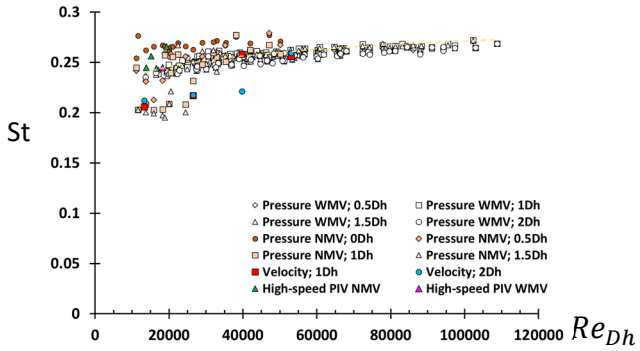

Figure 6: Strouhal-Reynolds Map

device. For the cross-correlation method, the size of the correlation window is selected as 0.5sec, i.e. 10*f_{peak} which is observed to be sufficient to catch the periodicity in the flow for the presented case. Each selected window is then moved backward and forward along the entire PIV duration. For the cross-correlation Eq. (2) is used where R(τ) represents the correlation coefficient and τ represents the lag (sec) information. The pressure fluctuation, P', and the velocity fluctuation, V' are normalized with the root mean square (RMS) values per selected window and the result of cross-correlation is normalized by the standard deviation of each fluctuation. The final correlation coefficient is calculated by the mean R(τ) over all of the windows, i.e. over 4 sec of recording.

$$\mathrm{R}(\tau) = \frac{\overline{(P'(t) * V'(t+\tau))}}{\sigma_{P'(t)}\sigma_{V'(t+\tau)}} \tag{2}$$

The preliminary results are plotted as Figure 7 by using the normalized time phase $\tau^* = \tau U_{flow}/D_h$, and the distance between correlation points. The time shift between two signals is found by the maximum and the minimum peak point after the first zero crossing point of R(τ). These points which can be seen Figure 7(a) for one position, represents negative and positive lag of periodic cross-correlation results as, τ_- and τ_+respectively. Figure 7(b) shows position of cross-correlation between the second sensor, i.e. yellow circle, and the velocity points, i.e. z/Dh=0.2 and z/Dh=-0.2 for Re_{D_h}=20000. The slope of each linear result represents the convection velocity of the correlated structure. On Figure 7(c) and (d), each calculated slope is

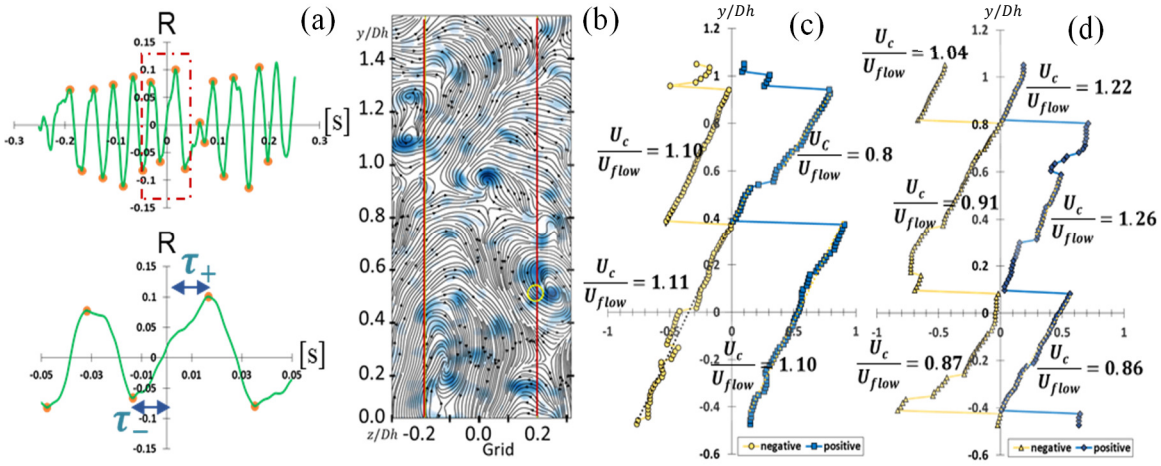

Figure 7: (a) Cross-correlation result with zoom-in (b)Position of selected velocity data and the pressure sensor which are represented with red lines and yellow circle, respectively (c) results for x/Dh=0.2 (d) time shift results for x/Dh=-0.2

shown as $U_c \ / \ U_{flow}$ where U_{flow} is 0.9 m/s. The mean of dimensionless convection velocity is calculated as 1.03±0.15. This shows that the structures are transported by the mean flow with 15% variations. The variation on the $\overline{(U_c)}$, i.e. standard deviation might be due to the contraction after the grid which creates inhomogeneous velocity field.

4 CONCLUSIONS

The PIV measurements are performed with different distances, velocities and temperatures for WMV and NMV. The coherent structures are observed to persist at least up to 1.4Dh for both configuration. Using time resolved velocity data for NMV configuration, two different time scales are estimated and connected to length-scales by using U_{flow}. The integral length scale represent the size of the coherent structures and the periodic length scale represents the distance between two periodic structures. The structures that are presented with swirling function show coherent length scales for both high and low Reynolds numbers. This shows the connection between the structures and the velocity fluctuations. Strouhal-Reynolds map is built according to the frequency peak on spectra and the results shows that the phenomena is represented by the coherent structures for both pressure fluctuations and velocity fluctuations. Transport of velocity and pressure fluctuations are investigated with simultaneous measurements by using multisensor pressure device and PIV for NMV configuration. The results show that the structures are transported by the mean flow downstream the grids, with 15% variations which is the local spatial oscillation of velocity profiles.

REFERENCES

[1] N. Turankok, S. Moreno, F. Bazin, V. Biscay, T. Lohez, D. Picard, S. Testanière and L. Rossi, "Unsteady pressure and velocity measurements in 5x5 rods bundle using grids with and without mixing vanes," Nuclear Engineering and Design, vol. 364, p. 110687, 2020.

[2] N. Turankok, T. Lohez, F. Bazin, V. Biscay and L. Rossi, “Exploration of Frequencies Peaks Observed On Local Wall Pressure Measurements by Time Resolved Velocity Fields Measurements in Complex Flows,” Experiments in Fluids, vol. 62, p. 38, 2021.

[3] R. E. Masterson, Nuclear Reactor Thermal Hydraulics - An Introduction to Nuclear Heat Transfer and Fluid Flow, Boca Raton: CRC Press, 2019.

[4] International Atomic Energy Agency, “Review of Fuel Failures in Water Cooled Reactors, Nuclear Energy Series No. NF-T-2.1,” IAEA, Vienna, Austria, 2010.

[5] J. Xiong, N. Yu, Y. Yu, X. Fu, X. Cheng and Y. Yang, "Experimental investigation on anisotropic turbulent flow 6x6 rod bundle with LDV," Nuclear Engineering and Design , vol. 278, pp. 333-343, 2014.

[6] M. E. Conner, Y. A. Hassan and E. E. Dominguez-Ontiveros, “Hydraulic benchmark data for PWR mixing vane grid,” Nuclear Engineering and Design, vol. 264, pp. 97-102, 2013.

[7] P. Qi, P. Wang, S. Hao, K. Cheng, S. Qiao and S. Tan, “Experimental study of flow structures in a large range downstream the spacer grid in a 5 × 5 rod bundle using TR-PIV,” International Journal of Heat and Fluid Flow, vol. 84, p. 108619, 2020.

[8] M. C. Gauffre, S. Benhamadouche and P. B. Badel, “Wall-Modeled Large Eddy Simulation of the Flow Through PWR Fuel Assemblies at ReH=66 000—Validation on CALIFS Experimental Setup,” Nuclear Technology, vol. 206, pp. 255-265, 2020.

[9] I. Zadrazil and C. N. Markides, "An experimental characterization of liquid films in downwards co-current gas-liquid annular flow by particle image and tracking velocimetry," International Journal of Multiphase Flow, vol. 67, pp. 42-53, 2014.

[10] B. Moudjed and L. Rossi, “Processing tools to track and charaterize surface swirls,” Journal of Flow Visualization and Image Processing, vol. 26, pp. 1-17, 2019.